ELSEVIER

Liquid phase epitaxy growth and characterization of $Ga_{1-x}In_xAs_ySb_{1-y}$ quaternary alloys

V. Rakovics [a,*], A.L. Tóth [a], B. Podör [a], C. Frigeri [b], J. Balázs [a], Z.E. Horváth [a]

[a] *Hungarian Academy of Sciences, Research Institute for Technical Physics and Materials Science, Konkoly-Thege út 29-33, 1121 Budapest, Hungary*
[b] *CNR MASPEC Institute, Parco Area delle Scienze 37/A, Fontanini, 43010 Parma, Italy*

Abstract

Band gap, solid phase composition and lattice mismatch data are presented characterising $Ga_{1-x}In_xAs_ySb_{1-y}$ layers grown by liquid phase epitaxy (LPE) on $\langle 100 \rangle$ oriented GaSb substrate. Nearly lattice-matched ($|\Delta a/a| < 0.15\%$) $Ga_{1-x}In_xAs_ySb_{1-y}$ layers were grown over the range $0 < x < 0.20$. The lattice-mismatch was estimated from X-ray diffraction measurements. The X-ray diffraction pattern of the lowest band gap (0.55 eV) $Ga_{0.80}In_{0.20}As_{0.17}Sb_{0.83}$ layer showed strong compositional grading, indicating the presence of a miscibility gap near this composition in this material system. The composition of the grown epitaxial layers was determined by electron probe microanalysis in the wavelength dispersive mode. Band gap energies down to 0.55 eV were obtained on different composition samples from infrared transmission measurements. The measured compositional dependence of the band gap exhibits smaller bowing than calculated using the correlated function expansion technique. © 2002 Elsevier Science B.V. All rights reserved.

Keywords: Liquid phase epitaxy; GaInAsSb; X-ray diffraction; X-ray microanalysis

1. Introduction

Antimonide-based compound semiconductors have received much attention for their application in photonic devices over a wide spectral range from 1240 nm (AlGaAsSb) [1] to 4200 nm (GaInAsSb) [2]. AlGaAsSb and GaInAsSb can be grown lattice matched to GaSb and InAs substrates by liquid phase epitaxy (LPE) [3–9]. The band gap of the solid solutions can be altered by varying the composition of the solid phase of the epitaxial layer. Detailed knowledge of the band gap and lattice constant for this quaternary alloy are important for many practical applications. Both theoretical predictions and experimental evidence point to the existence of a miscibility gap in $Ga_{1-x}In_xAs_ySb_{1-y}$. This quaternary alloy may provide the basis for devices such as light-emitting diodes, lasers, photodetectors and thermophotovoltaic energy converters [10–13]. In this paper, we report the LPE growth and characterisation

of $Ga_{1-x}In_xAs_ySb_{1-y}$ layers. Band gap energies from 0.726 eV (i.e. GaSb) to 0.55 eV were obtained from infrared transmission measurements. Unintentionally doped $Ga_{1-x}In_xAs_ySb_{1-y}$ layers were p-type for $x < 0.10$ and n-type for $x > 0.10$.

2. Experimental methods

$Ga_{1-x}In_xAs_ySb_{1-y}$ ($0 < x < 0.20$) layers were grown by liquid phase epitaxy (LPE) on $\langle 100 \rangle$ GaSb:Te ($n \approx 10^{18}$ cm^{-3}) substrates in a quartz reactor tube heated by a single-zone semi-transparent furnace. Single-phase growth solutions were prepared from 6 N In, Ga, Sb and from undoped ($n \approx 10^{15}$ cm^{-3}) GaAs. The melts were homogenised and purified for 2 h at 670 °C. After loading the wafer, and purging with purified hydrogen, the melt was heated to 630 °C for 1 h to completely dissolve the growth solution, then the temperature was quickly reduced to 530 °C. During further reduction of the temperature to 520 °C the cooling rate was kept constant. Prior to growth, the substrate was etched in situ with an undersaturated GaSb solution to remove

* Corresponding author. Tel.: + 36-1-392-2222/3532; fax: + 36-1-392-2237.

E-mail address: rakovics@mfa.kfki.hu (V. Rakovics).

Table 1
Summary of growth conditions (growth temperature T_g, growth time t, atomic fraction of the components in the liquid X^l) for different InGaAsSb layers

T_g (°C)	t (s)	X^l_{Ga}	X^l_{As}	X^l_{In}	X^l_{Sb}	λ_g (nm)
527–524.5	180	0.948			0.052	1708
527–525	120	0.4569	0.000399	0.3899	0.153	1933
529.5–526.5	120	0.3450	0.000587	0.4740	0.180	2008
528.5–525.5	120	0.2178	0.000912	0.5600	0.221	2126
528.8–525.9	120	0.2178	0.000912	0.5600	0.221	2129
528.7–527.7	120	0.1586	0.001204	0.5898	0.250	2202
529–528	120	0.1377	0.001398	0.6013	0.260	2254

the thin residual oxide layer from the GaSb surface. The epitaxial layer was grown by means of the supercooling technique. The growth conditions are summarised in Table 1. After the growth, the wafers were cleaned by etching off the melt residuals by hot HCl. In this study the various samples have been cleaved and stained with basic $K_3Fe(CN)_6$ for epitaxial layer thickness measurements. The layer thickness d was about 4–6 μm. Optical transmittance spectra were measured using a 100 W halogen lamp whose light was chopped and passed through a monochromator with a 1:8.4 aperture. The resolution was 8 nm. The transmitted light was detected by a PbS detector using lock-in techniques.

The lattice mismatch of the quaternary layers with respect to the GaSb substrate as determined by X-ray diffraction (Cu $K_{\alpha1}$ radiation, (400) Bragg reflection) was $|\Delta a/a| < 1.5 \times 10^{-3}$ (Table 2). The composition of the epitaxial layers was determined by an electron microprobe analyser (EMPA) in the wavelength dispersive mode (WDM) in a JEOL JSM 35 machine using the In L_α, Ga L_α, As L_α and Sb L_α lines. GaAs, InSb and GaSb single crystals were used as standards. The excitation electron energy was 15 keV. To obtain the composition, atomic number, absorption, and fluorescence (ZAF) corrections were performed. The uncertainties in x and y are less than ± 0.002.

Gold Schottky contacts were prepared on the quaternary layers. The free carrier concentration of the layers was determined by C–V measurements on GaInAsSb/Au Schottky diodes. On some samples the band gap wavelength of the quaternaries was also determined from the spectral response of the Schottky photodiodes.

3. Results and discussion

Thick (4–6 μm) mirror like $Ga_{1-x}In_xAs_ySb_{1-y}$ ($0 < x < 0.20$) layers, lattice matched to GaSb substrate, have been grown by LPE. As expected from Vegard's law the values of the composition ratio y/x are approximately equal to 0.9 for the near lattice matched quaternary layers. Fig. 1 shows the plot of the composition
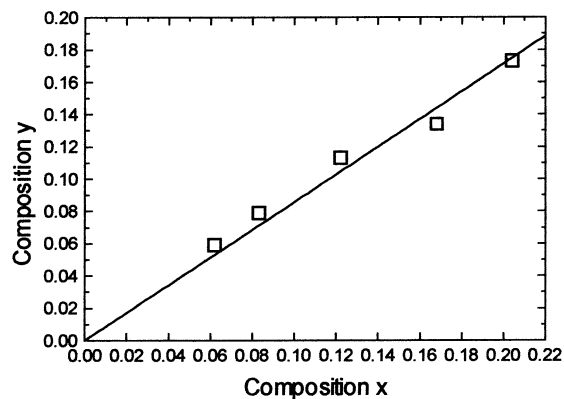
parameters y versus x as determined from EMPA. The straight line is the best fit with a slope corresponding to $y/x = 0.87 \pm 0.08$. The normalised transmittance spectra of GaSb (reference) and $Ga_{1-x}In_xAs_ySb_{1-y}$ layers listed in Table 2 are shown in Fig. 2. The band gap E_g was determined from the transmittance spectra using the relationship

$$\alpha = K(hv - E_g)^{1/2}/hv$$

The absorption coefficient α was calculated from the expression

Table 2
Band gap wavelength λ_g, layer thickness d, solid phase compositions x, y, lattice mismatch $\Delta a/a$ and band gap energy E_g data of the GaInAsSb layers

λ_g (nm)	d	x	y	$\Delta a/a$ (%)	E_g (eV)	y/x
1708	15.7				0.726	
1832		0.043			0.667	
1933	5.7	0.062	0.059	−0.1	0.641	0.945
2008	3.8	0.083	0.079	−0.12	0.618	0.948
2126	6.2	0.122	0.113	−0.14	0.583	0.930
2129	5.9	0.123	0.112	−0.02	0.582	0.916
2202	6.1	0.168	0.134	0.05	0.563	0.798
2254	4.1	0.204	0.173	0.07	0.550	0.85

Fig. 1. Plot of the composition parameters y vs. x as determined from EMPA. The straight line is the best fit with a slope corresponding to $y/x = 0.87 \pm 0.08$.
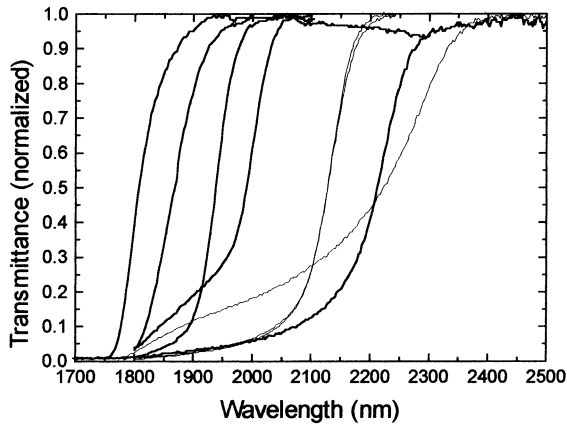
Fig. 2. Normalised transmittance spectra of the quaternary alloys. Curves from left to right: GaSb (reference), $In_xGa_{1-x}As_ySb_{1-y}$ with $x = 0.043$, 0.062, 0.083, 0.122, 0.123, 0.168, and 0.204.
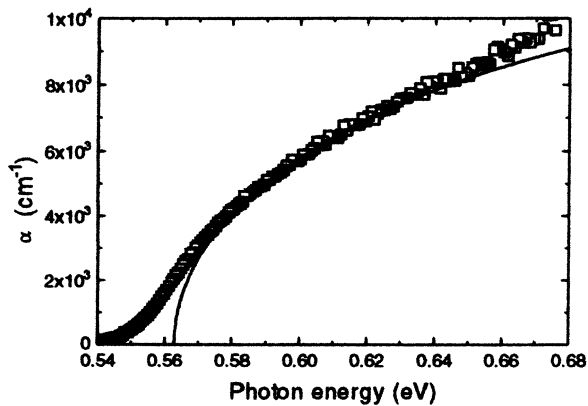

Fig. 3. Near band edge absorption coefficient of $In_xGa_{1-x}As_ySb_{1-y}$ ($x = 0.168$). The line represents the fitted curve $\alpha \sim (hv - E_g)^{1/2}/hv$ with $E_g = 0.563$ eV.
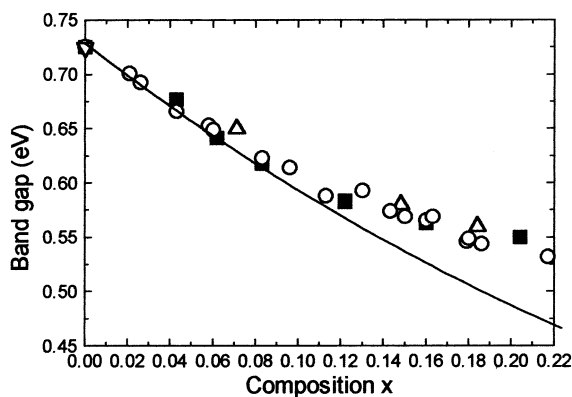

Fig. 4. Band gap of the quaternary alloy vs. the composition x. Solid squares — this work; open circles — DeWinter et al. [4]; up triangles — Astles et al. [3]; down triangle — data for GaSb. Full line-semi empirical curve based on the CFE model, Shim et al. [14].

$$I_t/I_0 = (1 - R)^2 \exp(-\alpha d)/[1 - R^2 \exp(-\alpha d)]$$

which takes into account multiple internal reflections. Here R is the reflection coefficient, d the sample thick-

ness, and I_t/I_0 the ratio of transmitted to incident intensity. In view of the relatively small range of composition x and noting the absence of experimental data for the quaternary alloy $Ga_{1-x}In_xAs_ySb_{1-y}$ the reflection coefficient was taken as $R = 0.345$, i.e. the value of GaSb. Fig. 3 shows the near band edge absorption coefficient of $Ga_{1-x}In_xAs_ySb_{1-y}$ ($x = 0.168$). The line represents the fitted curve $\alpha \sim (hv - E_g)^{1/2}/hv$ with $E_g = 0.563$ eV. The K coefficient in $\alpha = K(hv - E_g)^{1/2}/hv$ decreased with increasing x. The band gap is plotted versus the composition x in Fig. 4. In this figure solid squares represent this work, open circles are the data from DeWinter et al. [4], up triangles are the data from Astles et al. [3], and the down triangle represents the band gap of data for GaSb. The full line is the semi empirical curve based on the correlation function expansion (CFE) model by Shim et al. [14]. The present data agree well with earlier results [3,4]. However all three experimental data sets indicate a smaller bowing than predicted by the recent correlation function expansion (CFE) model of Shim et al. [14]. From our experimental data and from the known band gap values of the end compounds (0.726 eV for GaSb and 0.298 eV for $InAs_{0.91}Sb_{0.09}$, respectively) the bowing parameter for the quaternary alloy $Ga_{1-x}In_xAs_ySb_{1-y}$, lattice matched to GaSb is estimated as 0.71 ± 0.06 eV.

The discrepancy between the experimental results and the CFE calculation might have several reasons. The CFE model uses the experimental band gap data of the ternaries as inputs. The ternaries might have different microscopic structure and defects due to the different growth conditions. Furthermore the experimental data for the quaternary might be influenced by the effects of structural changes with increasing x as the boundary of immiscibility near $x \approx 0.2$ is being approached. Near and below the fundamental absorption edge an exponential absorption tail spanning a range of α values exceeding an order of magnitude (from below 100 to above 1000 cm^{-1}) corresponding to the Urbach's rule

$$\alpha = \alpha_0 \exp[(hv - E_g)/E_0]$$

was observed. The analysis of the experimental data resulted in values of $E_0 = 5–10$ meV for the Urbach parameter. While a detailed analysis of the behaviour of the Urbach parameter E_0 for various alloy compositions is yet needed, the presence of the exponential absorption tail in the present material system can most plausibly be ascribed to the effects of the random potential due to the alloy disorder.

The unintentionally doped $Ga_{1-x}In_xAs_ySb_{1-y}$ layers were p-type for $x < 0.10$ and n-type for $x > 0.10$. The free carrier concentration, evaluated from the $C–V$ measurement on Schottky diodes, was $p = 3 \times 10^{17}$ for $x = 0$, (GaSb) and $n = 1.2 \times 10^{17}$ for GaInAsSb ($x =$

0.204). Closer inspection of Fig. 2 shows that the absorption edge of our n-type GaInAsSb ($x > 0.10$) has a blue shift compared to p-type samples from the literature, which is thought to be the Moss–Burstein shift. The calculated blue shift for n-type (1.2×10^{17}) sample was 20 meV, similar to the experimental value (16 meV).

The spectral response of Schottky photodiode is also suitable for the band gap determination.

4. Conclusions

We have studied the optical properties of $Ga_{1-x}In_xAs_ySb_{1-y}$ ($y/x \approx 0.9$, $0 < x < 0.20$) layers lattice matched to GaSb substrate. The measured band gaps as a function of the composition x are in good agreement with previous data from the literature, the bowing being smaller than predicted by the correlated function expansion model. The K coefficient in $\alpha = K(hv - E_g)^{1/2}/hv$ decreased with increasing x.

Below the fundamental absorption edge an exponential absorption tail (Urbach's rule) was observed which is tentatively ascribed to the effects of the random potential due to the alloy disorder.

Acknowledgements

References

[1] A. Sasaki, M. Nishiuma, Y. Takeda, Jpn. J. Appl. Phys. 19 (1980) 1695.
[2] T.H. Chiu, J.L. Zyskind, W.T. Tsang, J. Electron. Mater. 16 (1987) 57.
[3] M. Astles, H. Hill, A.J. Wiliams, P.J. Wrigth, M.L. Joung, J. Electron. Mater. 15 (1986) 41.
[4] J.C. DeWinter, M.A. Pollack, A.K. Srivastava, J.L. Zyskind, J. Electron. Mater. 14 (1985) 729.
[5] A.E. Bocharev, V.N. Gul'gazov, L.M. Dolginov, A.A. Semin, Izv. Akad. Nauk SSSR Nearg. Mater. 23 (1987) 1610.
[6] R. Sankaran, G.A. Antypas, J. Cryst. Growth 36 (1976) 198.
[7] F. Kaoruta, A. Marbeuf, A. Joullie, J.H. Fan, J. Cryst. Growth 79 (1986) 445.
[8] E. Tourine, F. Pitard, A. Joullie, A. Fourcade, J. Cryst. Growth 104 (1990) 683.
[9] N. Kobayashi, Y. Horikoshi, C. Uemura, Jpn. J. Appl. Phys. 18 (1979) 2169.
[10] Yu.P. Yakovlev, A.N. Baranov, A.N. Imenkov, M.P. Mikhailova, SPIE 1510 (1991) 120.
[11] J.P. van der Ziel, T.H. Chiu, W.T. Thang, J. Appl. Phys. 60 (1986) 4087.
[12] C. Caneau, J.L. Zyskind, J.W. Sulhoff, T.E. Glover, J.C. Centanni, J.C.A. Burrus, A.G. Dentai, M.A. Pollack, Appl. Phys. Lett. 51 (1987) 764.
[13] J.L. Zyskind, J.C. DeWinter, J.C.A. Burrus, J.C. Centanni, A.G. Dentai, M.A. Pollack, Electron. Lett. 25 (1989) 568.
[14] K. Shim, H. Rabitz, P. Dutta, J. Appl. Phys. 88 (2000) 7157.